S1 Partial correlation analysis

To isolate the relationship between the Dipole Mode Index (DMI) and the principal components (PC1 and PC2) of MHW intensity from the influence of ENSO, we computed the partial correlation controlling for Niño3.4. The partial correlation coefficient was calculated using the standard formula:

$$r_{xy \cdot z} = \frac{r_{xy} - r_{xz} r_{yz}}{\sqrt{(1 - r_{xz}^2)(1 - r_{yz}^2)}} \tag{S1}$$

where r_{xy} is the Pearson correlation between DMI (x) and PC (y), r_{xz} between DMI and Niño3.4 (z), and r_{yz} between PC and Niño3.4. This quantifies the direct association between DMI and PC after removing the linear influence of Niño3.4.

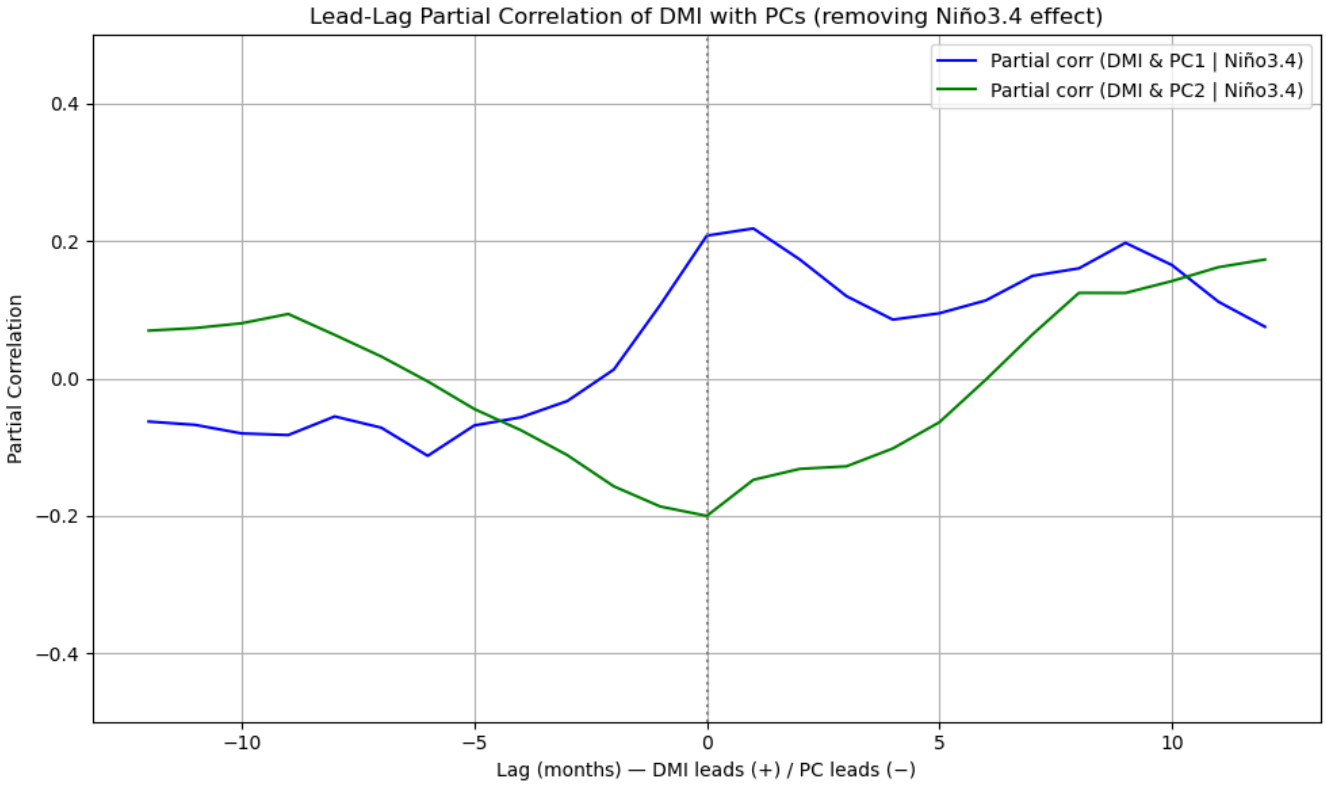

Fig. S1. Lead–lag partial correlation between the Dipole Mode Index (DMI) and the principal component time series (PC1 and PC2) of daily marine heatwave intensity in the North Indian Ocean, after removing the influence of Niño3.4 (ENSO).

Table S1. Extreme MHW Mode 1 Events During JJAS. Events were selected based on PC time series exceeding the seasonally varying 90th percentile for at least 5 consecutive days during the JJAS season.

No.	Start Date	End Date	Duration (days)
1	05-Jun-1982	10-Jun-1982	6
2	21-Sep-1982	26-Sep-1982	6
3	24-Jun-1983	21-Aug-1983	59
4	26-Aug-1983	03-Sep-1983	9
5	22-Jul-1987	21-Aug-1987	31
6	09-Jul-1988	14-Jul-1988	6
7	24-Jul-1988	01-Aug-1988	9
8	03-Jul-1993	07-Jul-1993	5
9	12-Sep-1997	23-Sep-1997	12
10	18-Jul-1998	08-Sep-1998	53
11	28-Aug-2005	06-Sep-2005	10
12	19-Jun-2006	24-Jun-2006	6
13	16-Jul-2010	20-Jul-2010	5
14	21-Aug-2015	19-Sep-2015	30
15	15-Aug-2023	15-Sep-2023	32
16	09-Jun-2024	29-Jun-2024	21

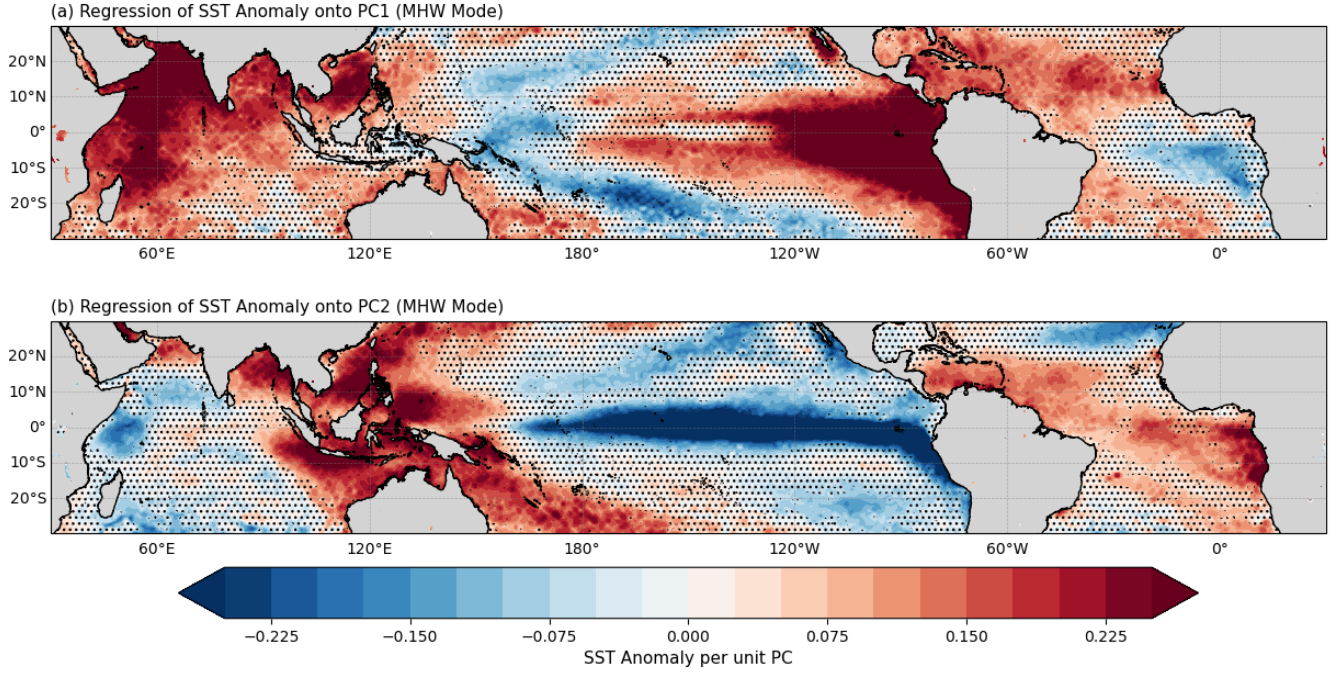

Fig. S2. Regression between SST and (a) PC1 time series and (b) PC2 time series.

Table S2. Extreme MHW Mode 2 Positive Events During JJAS. Events were selected based on PC 2 time series exceeding the seasonally varying 90th percentile for at least 5 consecutive days during the JJAS season.

No.	Start Date	End Date	Duration (days)
1	08-Aug-1982	12-Aug-1982	5
2	11-Jun-1983	23-Jun-1983	13
3	13-Sep-1983	29-Sep-1983	17
4	26-Jun-1987	07-Jul-1987	12
5	03-Aug-1988	22-Aug-1988	20
6	30-Aug-1988	20-Sep-1988	22
7	07-Jul-1991	17-Jul-1991	11
8	06-Jun-1992	15-Jun-1992	10
9	08-Jul-1993	13-Jul-1993	6
10	29-Jul-1993	03-Aug-1993	6
11	09-Aug-1993	15-Aug-1993	7
12	08-Jul-1996	15-Jul-1996	8
13	20-Jul-1996	24-Jul-1996	5
14	18-Aug-1996	23-Aug-1996	6
15	14-Jun-1998	07-Jul-1998	24
16	18-Sep-2001	23-Sep-2001	6
17	14-Jun-2002	22-Jun-2002	9
18	29-Jun-2002	23-Jul-2002	25
19	14-Jun-2005	23-Jun-2005	10
20	28-Jun-2005	04-Jul-2005	7
21	13-Jul-2005	24-Jul-2005	12
22	19-Jun-2007	24-Jun-2007	6
23	25-Jul-2007	02-Aug-2007	9
24	09-Jun-2010	15-Jun-2010	7
25	17-Aug-2010	30-Aug-2010	14
26	26-Aug-2016	30-Aug-2016	5
27	09-Sep-2017	15-Sep-2017	7
28	01-Jul-2020	09-Jul-2020	9
29	17-Jul-2020	17-Aug-2020	32
30	22-Aug-2020	25-Sep-2020	35
31	03-Jun-2021	07-Jun-2021	5
32	27-Jul-2022	07-Aug-2022	12
33	29-Aug-2022	08-Sep-2022	11
34	13-Aug-2024	22-Aug-2024	10

Table S3. Extreme MHW Mode 2 Negative Events During JJAS. Events were selected based on PC 2 time series falling below the seasonally varying 10th percentile for at least 5 consecutive days during the JJAS season.

No.	Start Date	End Date	Duration (days)
1	21-Jun-1982	28-Jul-1982	38
2	27-Aug-1982	31-Aug-1982	5
3	04-Jun-1983	08-Jun-1983	5
4	10-Sep-1987	25-Sep-1987	16
5	17-Jun-1988	21-Jun-1988	5
6	18-Aug-1990	22-Aug-1990	5
7	03-Jul-1992	14-Jul-1992	12
8	18-Jul-1992	22-Jul-1992	5
9	29-Jun-1995	04-Jul-1995	6
10	06-Jun-1997	03-Jul-1997	28
11	10-Jul-1997	22-Jul-1997	13
12	04-Jun-1998	10-Jun-1998	7
13	24-Aug-2006	11-Sep-2006	19
14	17-Jun-2009	02-Jul-2009	16
15	22-Sep-2009	27-Sep-2009	6
16	05-Aug-2011	19-Aug-2011	15
17	21-Jul-2012	25-Jul-2012	5
18	29-Jul-2012	14-Aug-2012	17
19	03-Sep-2013	08-Sep-2013	6
20	02-Aug-2015	07-Aug-2015	6
21	14-Sep-2018	19-Sep-2018	6
22	05-Jul-2024	13-Jul-2024	9

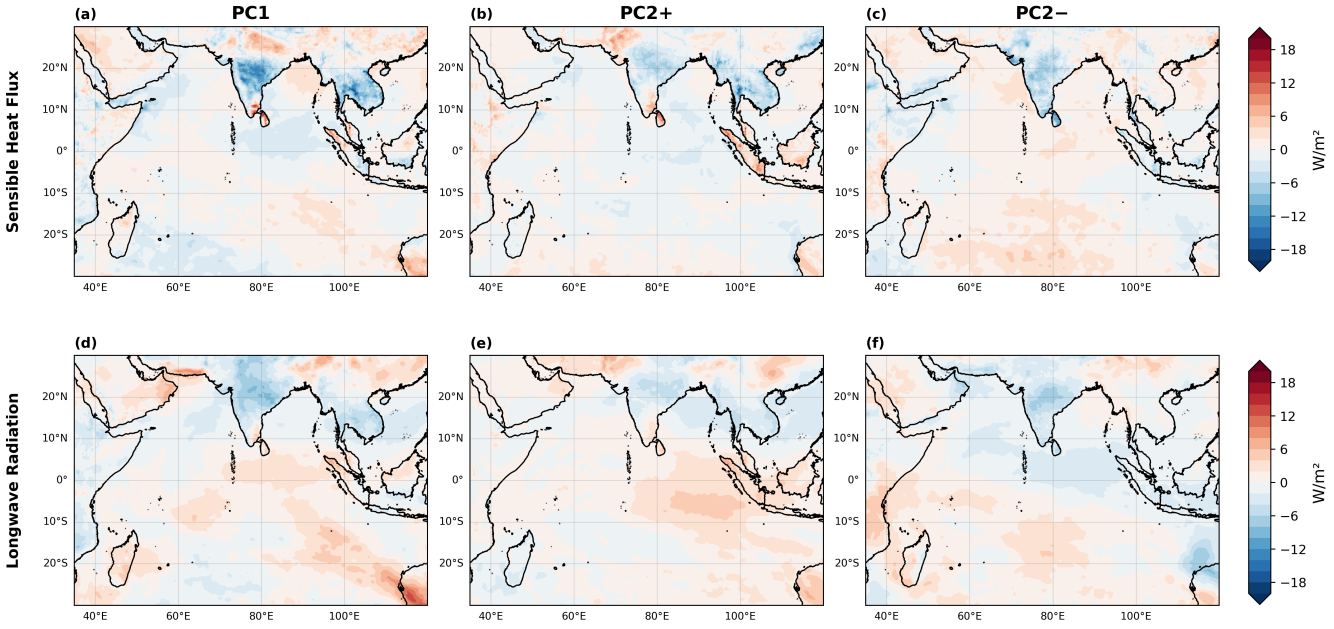

Fig. S3. Composite anomalies averaged over the 5 days preceding MHW onset for the PC1 mode (left), PC2-positive mode (middle), and PC2-negative mode (right). Rows show: (1) sensible heat flux anomaly (W/m^2), (2) longwave radiation anomaly (W/m^2).

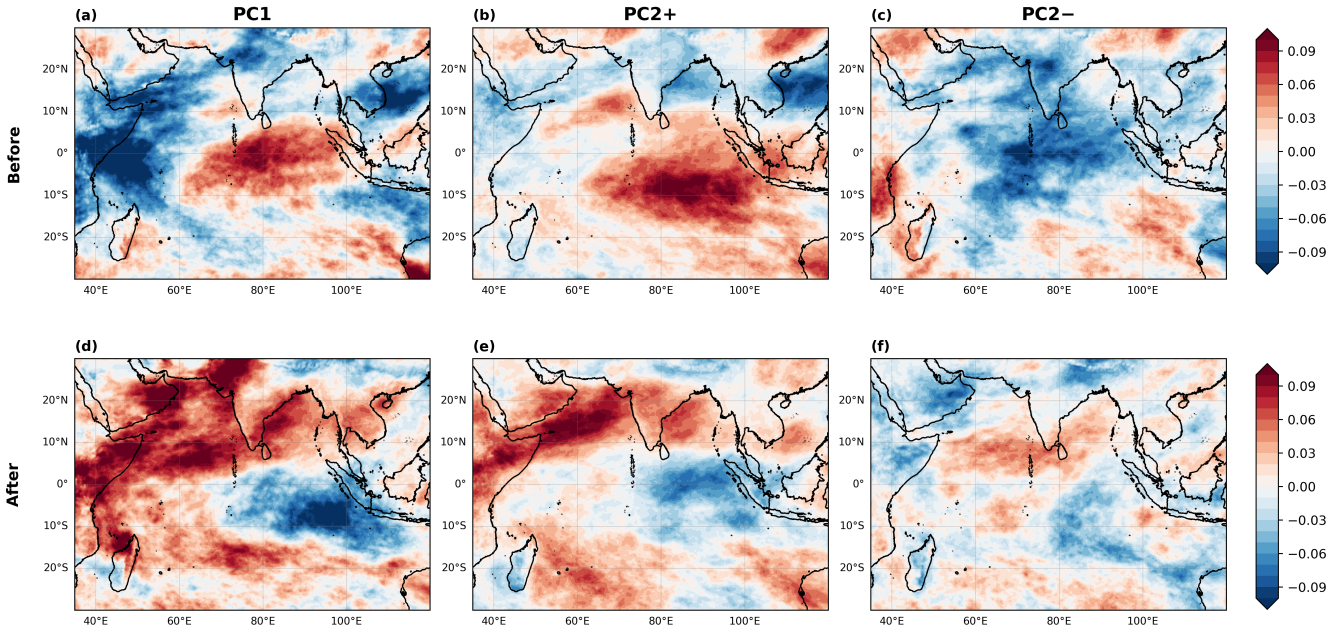

Fig. S4. Composite anomalies of total cloud cover (fraction) averaged over the 5 days preceding MHW onset (top) and 5 days after MHW termination (bottom) for the PC1 mode (left), PC2-positive mode (middle), and PC2-negative mode (right).

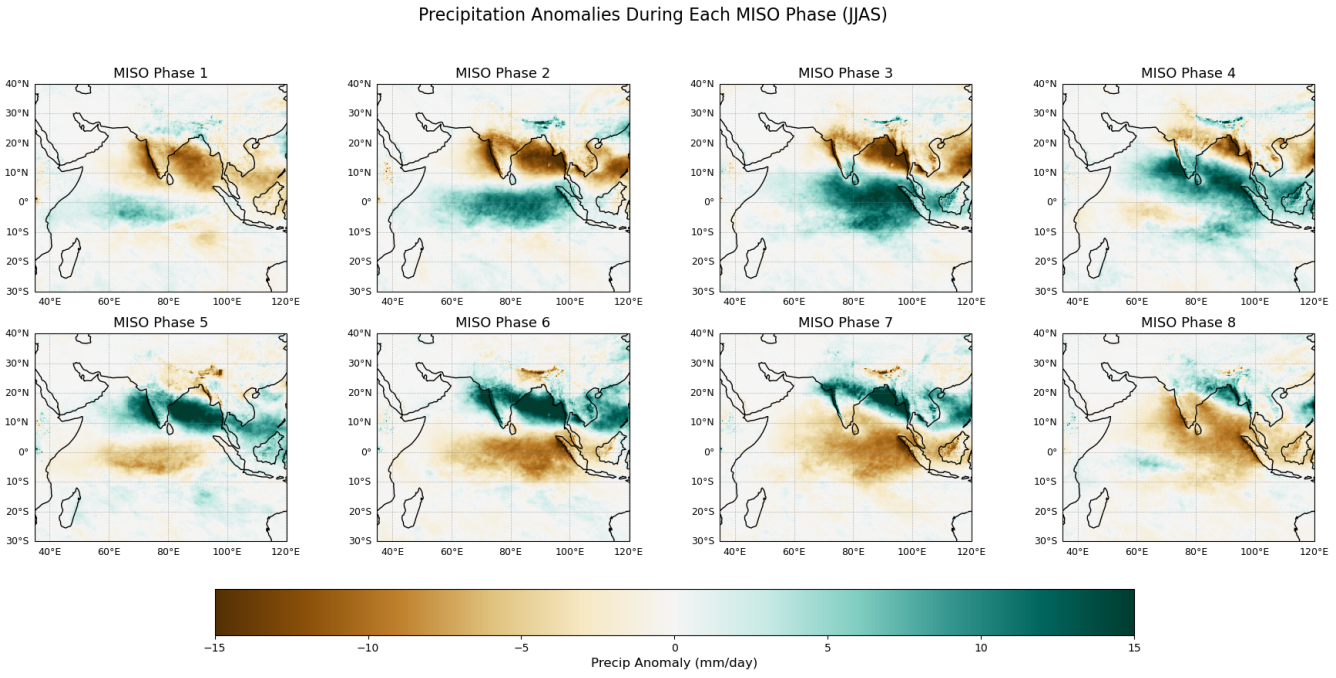

Fig. S5. Composite anomalies of precipitation during MISO phases.

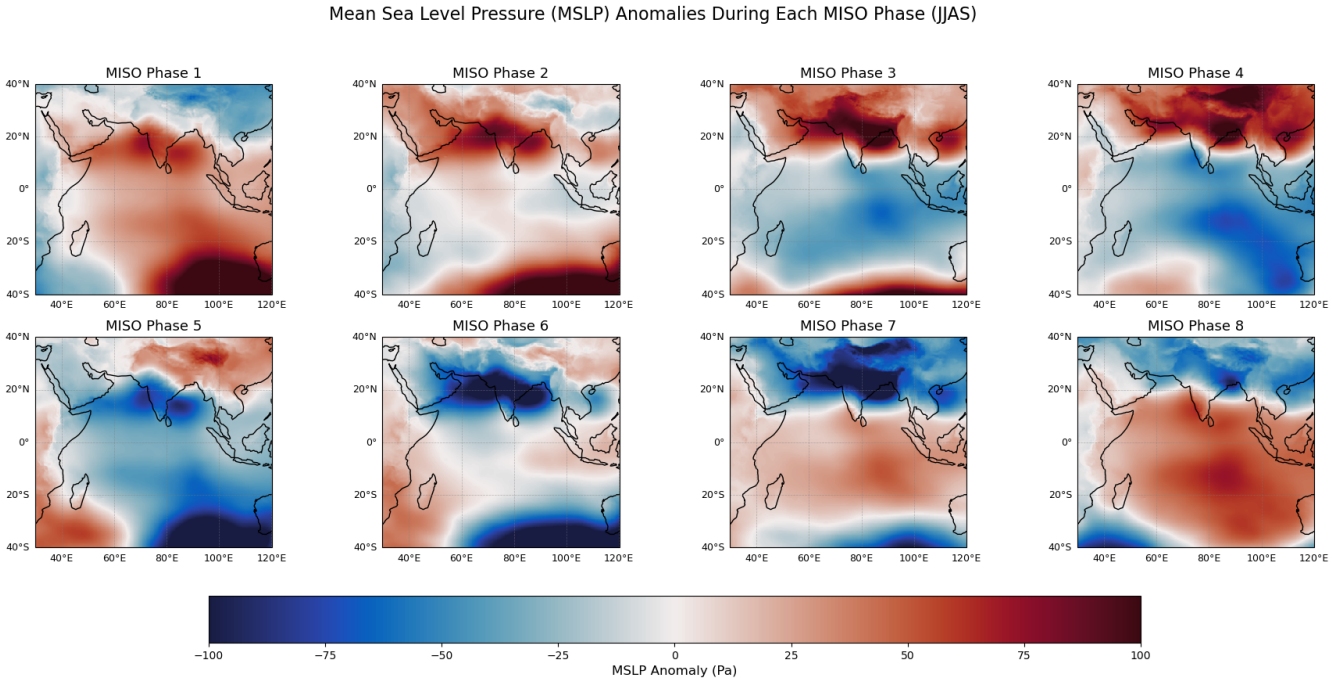

Fig. S6. Composite anomalies of mean sea level pressure during MISO phases.

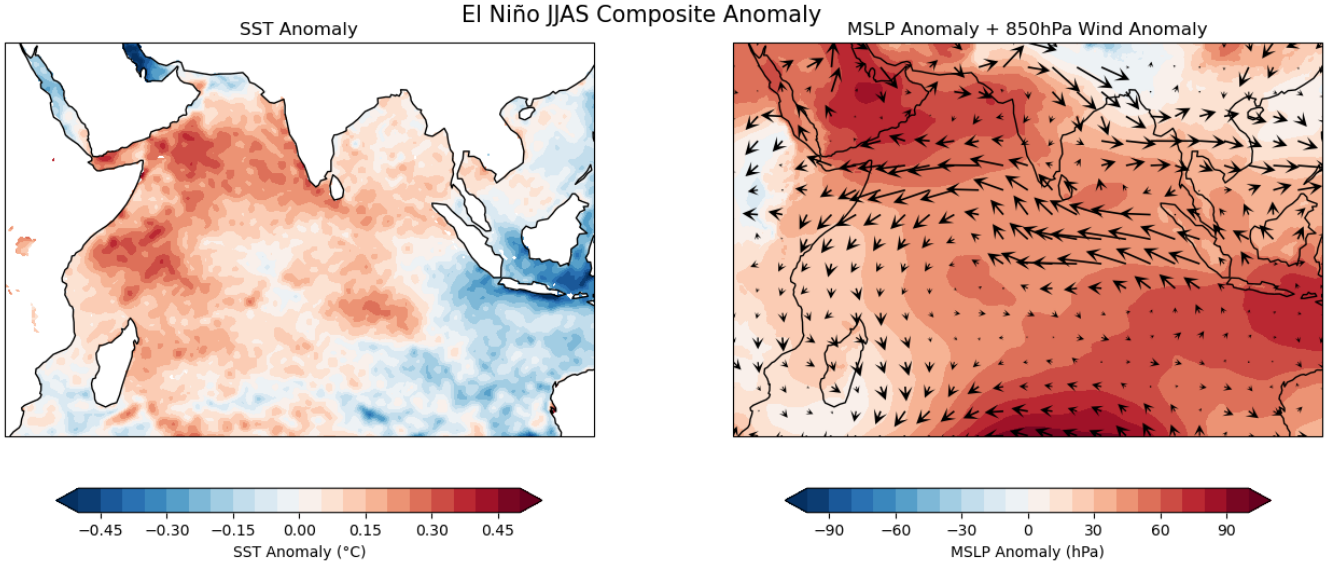

Fig. S7. Composite anomalies of SST, mean sea level pressure, and 850-hPa winds during El Niño years (JJAS).

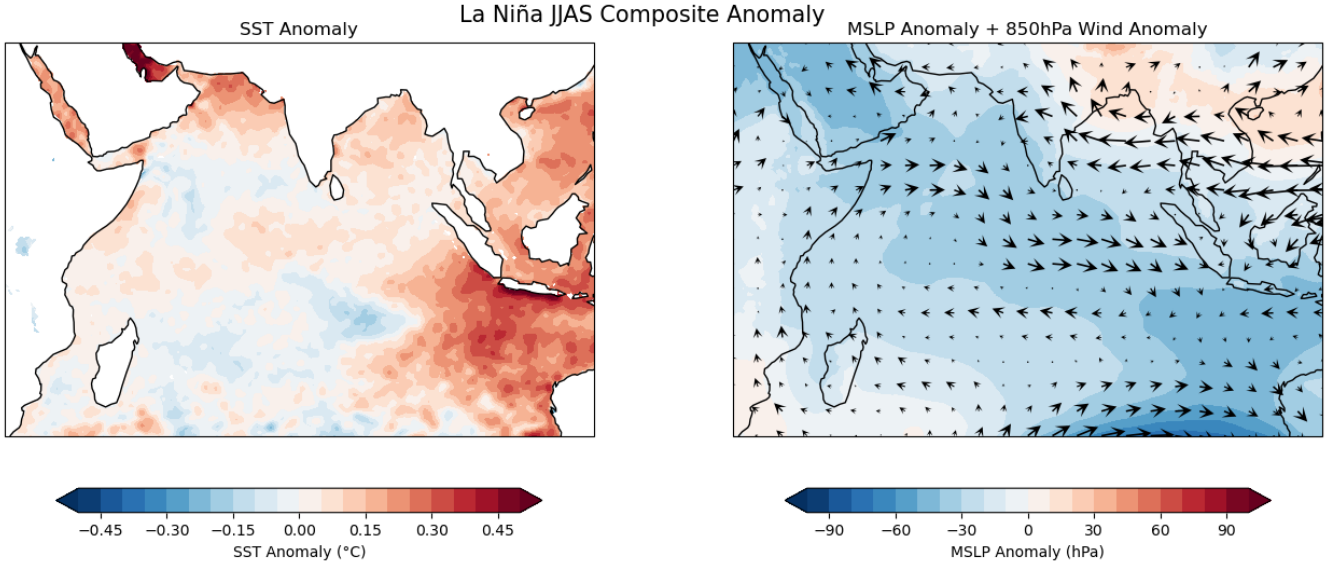

Fig. S8. Composite anomalies of SST, mean sea level pressure, and 850-hPa winds during La-Nina years (JJAS).

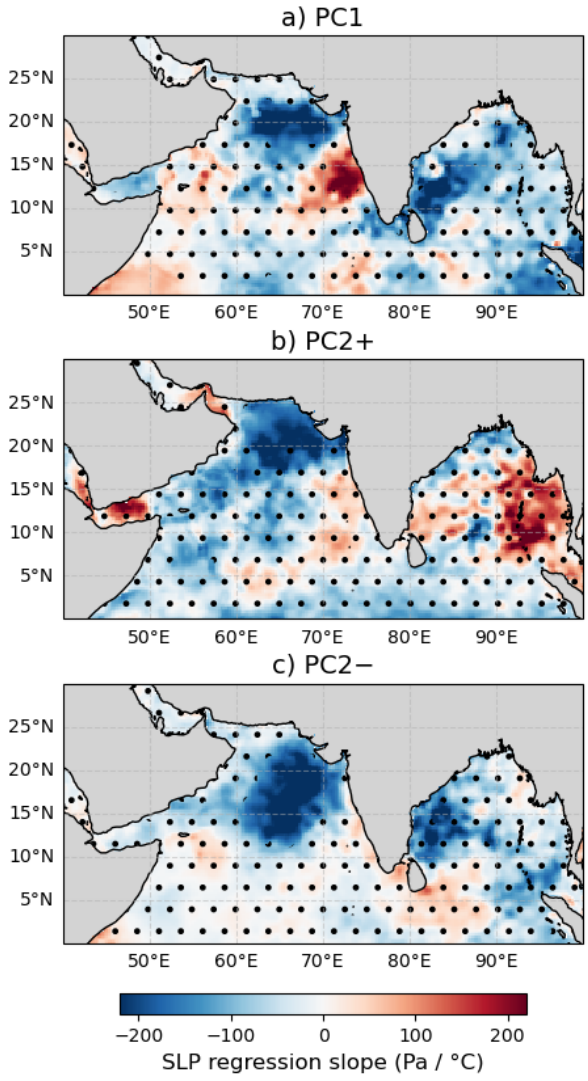

Fig. S9. Linear regression coefficients between SST and MSLP associated with the three different MHW modes: (a) PC1, (b) PC2+, and (c) PC2-. The regression is based on SST averaged over the 5 days preceding the end of each MHW event and MSLP averaged over the 5 days following the end of each MHW event. Hatching indicates regions where the regression is not statistically significant at the 90% confidence level.

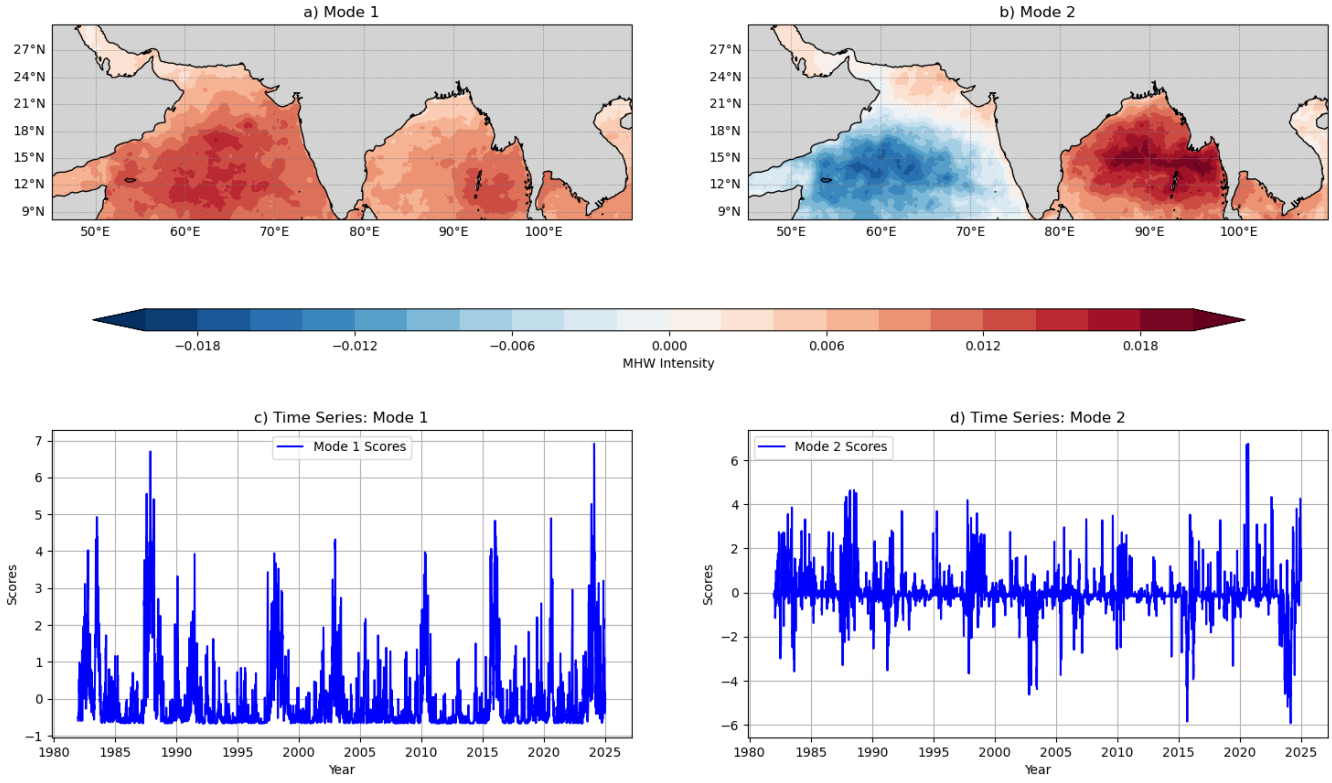

Fig. S10. Empirical Orthogonal Function (EOF) analysis of the MHW intensity in the North Indian Ocean using OISST SST. (a) Spatial pattern of the leading mode (Mode 1). (b) Spatial pattern of the second mode (Mode 2). (c) Normalized principal component time series corresponding to Mode 1. (d) Normalized principal component time series corresponding to Mode 2. Same as Figure 2 in the main text, but using SST from OISST.

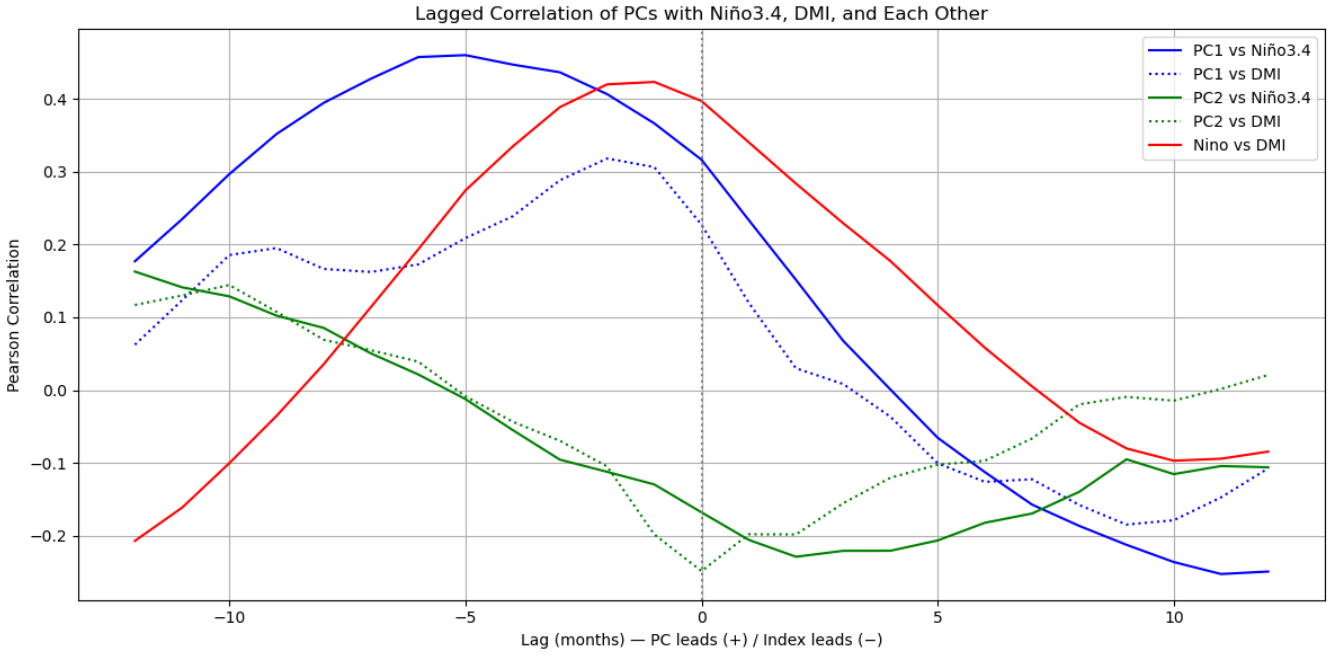

Fig. S11. Lead-lag correlations between the PCs (converted to monthly) and climate indices. Blue and green lines represent correlations involving PC1 and PC2, respectively. Solid lines denote correlations with Niño 3.4, while dashed lines denote correlations with the DMI. The red line shows the correlation between Niño 3.4 and DMI. Negative lags indicate the climate index leads the PC, while positive lags indicate the PC leads the index. Same as Figure 3 in the main text, but using SST from OISST.

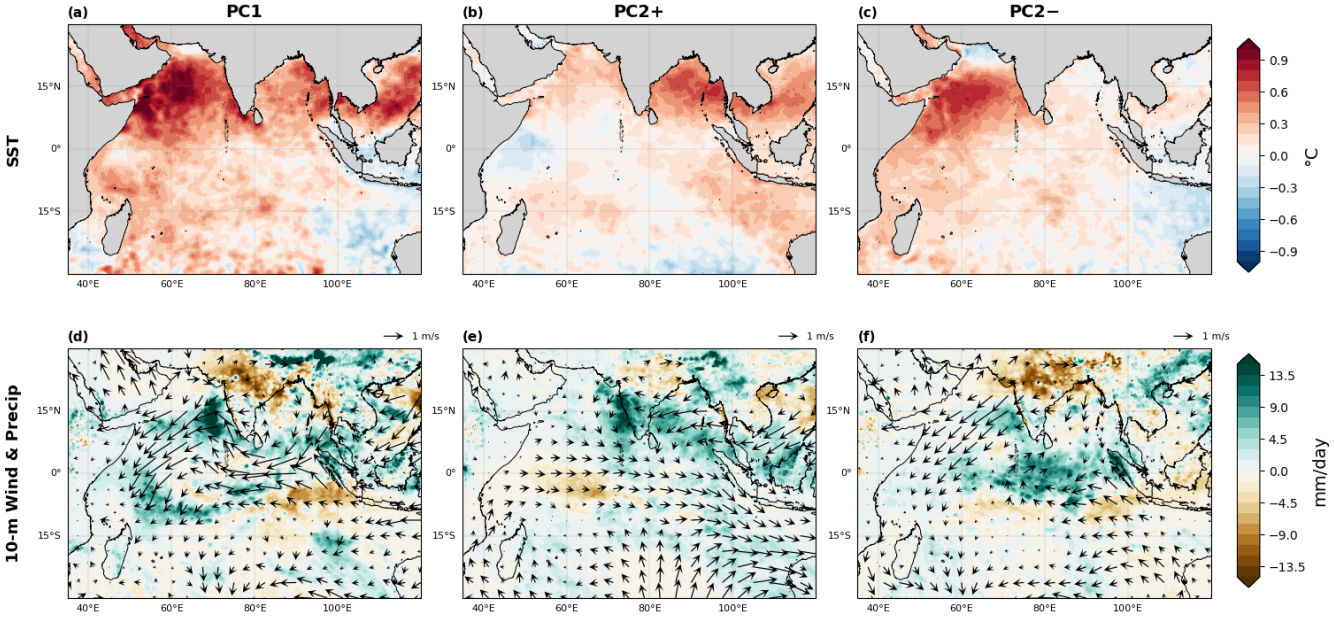

Fig. S12. Composite anomalies of (top row) SST (°C) and (bottom row) precipitation (shading; mm/day) and 10-meter wind vectors (arrows; m/s) during MHW events associated with PC1 (left), PC2+ (middle), and PC2- (right) phases. Same as Figure 4 in the main text, but using SST from OISST and selecting events based on PCs computed using OISST, following the same method as provided in the main text.